Plant Physiology and Biochemistry 138 (2019) 17–25

Contents lists available at ScienceDirect

Plant Physiology and Biochemistry

journal homepage: www.elsevier.com/locate/plaphy

Research article

Regulation by nitric oxide on mitochondrial permeability transition of peaches during storage

Dandan Huang[a,1], Shan Hu[b,1], Shuhua Zhu[a,*], Jianrong Feng[b]

[a] College of Chemistry and Material Science, Shandong Agricultural University, Taian, Shandong, 271018, China
[b] College of Agriculture, Shihezi University, Shihezi, Xinjiang, 832000, China

ARTICLE INFO

Keywords:
MMP
MPTP
Nitric oxide
Peach
PiC
VDAC

ABSTRACT

Mitochondrial membrane permeability transition pores (MPTP) play important roles in mitochondrial function. There are many chemicals in the mitochondria that can act as signal molecules to affect the membrane permeability of mitochondria and mediate to release various enzymes. As a signaling molecule, nitric oxide (NO) is a key player in fruit growth and development. However, the specific mechanism through NO regulates MPTP, and how exogenous NO prolongs fruit storage time are both unclear. In this study, Feicheng peaches were treated with different concentrations of exogenous NO (5, 15 and 30 μmol L^{-1}) and c-PTIO to determine the changes in mitochondrial membrane potential (MMP), hexokinase II activity, the contents of cytochrome C and Ca^{2+} in mitochondria, as well as the effects of voltage-dependent anion channels (VDAC) and phosphate carrier (PiC) proteins on MPTP during storage. The results showed that NO could form a 1:1 complex either with VDAC or PiC, which proved that NO could react with the protein of PiC or VDAC. Treatment with 15 μmol L^{-1} NO maintained stable mitochondrial Ca^{2+} content, and high potential and permeability of the mitochondrial membrane, while decreased cytochrome C content and increased hexokinase activity. When NO was removed, the opposite result appeared. These results indicated that exogenous NO could stabilize MMP and participate in MPTP regulation of peaches during storage.

1. Introduction

Mitochondria, the essential organelle in almost all eukaryotic cells with a bilayer membrane structure, are the primary site of ATP production. Mitochondrial membranes are a key focus in cellular physiology and respiratory energy pathways (Kühlbrandt, 2015). The mitochondrial structure consists of the mitochondrial outer membrane (MOM), the mitochondrial inner membrane (MIM) and the mitochondrial matrix. MOM is the main interface for exchanging various molecules with the surrounding cytosolic environment, as well as other organelles (Ellenrieder et al., 2017). Under physiological conditions, mitochondria undergo permanent swelling and then resulting in increased MIM permeability, when mitochondria are exposed to high concentrations of calcium. This disrupts chemical osmotic gradient of the entire MIM and is known as mitochondrial permeability transition. The resulting uncoupling of oxidative phosphorylation leads to a decrease in ATP production and an increase in reactive oxygen species (ROS) generation (Jing et al., 2016). Also, the MOM is commonly ruptured during swelling of mitochondria, which results in the release of cytochrome C that can trigger apoptosis.

Mitochondrial function is partially regulated by mitochondrial permeability transition pores (MPTP) (Perez and Quintanilla, 2017). MPTP is a highly conductive channel and the opening of the pore results in an increase in the permeability of the MIM and then can induce the loss of mitochondrial membrane potential, the impairment of cellular calcium homeostasis, oxidative stress, and a decrease in ATP production upon pathological activation (Perez and Quintanilla, 2017). MPTP is composed by different proteins, such as phosphate carrier (PiC), adenine nucleotide translocator (ANT), hexokinase, voltage-dependent anion channels (VDAC) and cyclophilin D (CyPD) (Perez and Quintanilla, 2017). Quickly opening of MPTP can lead to the depolarization of mitochondrial membrane, the production of ROS and the release of cytochrome C, and then promote the oxidative apoptosis of mitochondria (Wu et al., 2018). The main role of PiC is transporting inorganic phosphorus (Pi) to the mitochondrial matrix and Pi is one of the open factors that promote MPTP. MPTP inhibitors significantly inhibit the binding of PiC. It indicated that PiC is also involved in the mitochondrial formation and opening processes (Haferkamp and

---

[*] Corresponding author.
E-mail addresses: shuhua@sdau.edu.cn (S. Zhu), fengjr102@126.com (J. Feng).
[1] These authors contributed equally to this work.

https://doi.org/10.1016/j.plaphy.2019.02.020
Received 19 September 2018; Received in revised form 19 February 2019; Accepted 20 February 2019

Schmitz-Esser, 2012). VDAC plays a major role in mitochondria-mediated apoptosis, and mitochondrial calcium overload triggered by VDAC promotes the opening of MPTP (Tewari et al., 2015). Hexokinase plays a role in the protection of apoptosis and has a protective effect on MIM (Song et al., 2017). Hexokinase II (HKII) binds to the MOM with VDAC, which interacts with adenine nucleotide transposase (ANT) and forms a contact site between the outer and inner membranes. Cytochrome C is released into cytoplasm after mitochondrial permeability increased, which activates the cell death process (Tewari et al., 2015; Wang et al., 2017). Importantly, MPTP dysfunction is a critical factor for mitochondria-driven cell death (Perez and Quintanilla, 2017).

As a free radical inorganic signal molecule produced by a variety of mechanisms, NO has regulatory roles in various functional processes in biology (Bhattacharya et al., 2017; Yarlagadda et al., 2017). Plant mitochondria produce NO under hypoxic conditions through the action of cytochrome C oxidase and other electron transport chain components with nitrite (Igamberdiev et al., 2014). NO not only regulates the plant metabolism (i.e., plant cell signal transduction) but also controls the function of the mitochondria in the plant. That is, NO can affect mitochondrial respiration and electron transport chain at the level of cytochrome oxidase, modify the proteins in mitochondria, regulate the genes encoding mitochondrial proteins and play important effects in the production of ATP and induction of alternative oxidase of mitochondria, exhibiting its functional roles in plant mitochondrial metabolism (Gupta et al., 2016). NO can inhibit the respiratory rate and ethylene production of fruit, as well as promote the growth and development of plant seedlings (Domingos et al., 2015; Yu et al., 2014). The production of NO can be induced by cold stress, and NO *vice versa* regulates the signaling pathway of CBF in the plant (Sehrawat et al., 2013). NO can mediate a variety of physiological functions in plants, and delay fruit senescence by inhibiting the respiration and ethylene synthesis; also can regulate the activities of the antioxidant enzymes and the content of ROS to decrease the oxidative damage (Singh et al., 2009; Scheler et al., 2013; Correa-Aragunde et al., 2015). However, the role of NO in regulating MPTP of fruits during storage remains unclear.

In this study, Feicheng peaches were treated by different concentrations of NO solutions and 2-(4-carboxyphenyl)-4,4,5,5-tetramethylimidazoline-1-oxyl- 3-oxide (c-PTIO) solution as NO scavenger. The activity of mitochondrial hexokinase II and the concentrations of cytochrome C and Ca^{2+}, as well as the changes in potential and permeability of the mitochondrial membrane, were determined to explore the effects of NO on MPTP of peaches during storage.

2. Materials and methods

2.1. Materials and chemicals purchased

Peaches (*Prunus persica (L.)* Batsch, cv. Feicheng), at the physiological mature stage, were collected (Taian, Shandong, China) in the harvest season (July). They were selected for uniformity of size with the diameter about 85 mm and the pink color, and visually devoid of disease and mechanical damage. Before the treatment, peaches were stored at 0 °C for 24 h and divided into five groups randomly. Different concentrations of NO (0, 5, 15 and 30 $\mu mol\ L^{-1}$) and c-PTIO (5 $\mu mol\ L^{-1}$) were involved in this experiment. Each treatment was repeated three times with 100 peaches in each time, The peaches were dipped in the different solutions, respectively, for 10 min. After dried with air, the peaches were stored at 25 °C, relative humidity 80–85%.

2.2. Post-treatment analysis

2.2.1. Determination of firmness

The firmness of peaches was measured by the Edelberg GY-4 fruit firmness tester (Shanghai Shandu, China). The diameter of the probe was 11 mm, and the pressure peak was recorded. Nine fruit from each treatment were selected and tested individually. The results were expressed as $N\ cm^{-2}$.

2.2.2. Determination of soluble solids

The soluble solids content (SSC) of 9 fruits in each treatment were measured by a hand refractometer (Shanghai Cany Precision Instrument Co. Ltd, China), and expressed as °Brix.

2.2.3. Determination of cell membrane conductivity

Cell membrane permeability was measured by a DDS-307 precision conductivity meter (Shanghai Yidian Co. Ltd, China). Fifteen fruit discs (about 1 mm thick, 5 cm in diameter) were dipped in distilled water (40 mL), and the conductivity (P_0) was recorded immediately. After 10 min, the conductivity was recorded again as P_1. The discs were then boiled for 10 min (the solution was readjusted to the volume of 40 mL to offset the evaporation). When the solution cooled to ambient temperature, the final conductivity (P_2) was measured. The ratio of membrane conductivity was calculated by the following equation and expressed as %.

$$\text{Relative membrane permeability} = (P_1 - P_0)/(P_2 - P_0) \times 100\%$$

2.2.4. Determination of ethylene release

The determination of ethylene release was measured as described as Zhu et al. (2006). Ethylene was injected into a gas chromatograph (GC-9A, Shimadzu, Japan) that was equipped with a GDX-502 column and a flame ionization detector (FID). The rate of ethylene production was expressed as nmol $C_2H_4\ h^{-1}\ g^{-1}$ FW.

2.2.5. Determination of respiratory rate

The peaches (1000 g) were placed into a desiccator equipped with a rubber stopper and sealed at 25 °C for 2 h. The respiration rate was measured with a COMBO 280 O_2/CO_2 gas analyzer (manufactured in Italy), and expressed as mmol $CO_2\ kg^{-1}\ h^{-1}$ FW.

2.2.6. Determination of color

The color was detected using a CR-10 colorimeter (Konica Minolta, Japan). The changes in the surface of peaches samples were expressed as L* (whiteness or light/dark), a* (red/green) and b* (yellow/blue). The total color difference (ΔE*) were calculated using the following equations: $\Delta E^* = [(L^*)^2 + (a^*)^2 + (b^*)^2]^{1/2}$

2.2.7. Isolation and purification of mitochondria

Mitochondria were extracted and purified from peaches by differential and density-gradient centrifugation was described as Jing et al. (2016). The yield of purified mitochondria was assayed by detecting the activity of cytochrome *c* oxidase (Millar et al., 2001).

2.2.8. Determination of mitochondrial cytochrome C content

The content of mitochondrial cytochrome C was measured by the spectrophotometer (Margoliash and Frohwirt, 1959). The mitochondrial suspension (200 μL) was diluted to 2 mL with sonicated deionized water. After incubation at 37 °C for 5 min, 5 mg of sodium dithionite were added into the mixture. The mixture was mixed well and incubated at room temperature for 5 min. The content of mitochondrial cytochrome C was measured for absorbance at 520 nm by UV spectrophotometer (UV-2450, Shimadzu, Japan), which expressed as $\mu mol\ g^{-1}$ protein. A standard curve was used to calculate mitochondrial cytochrome C content of peaches.

2.2.9. Determination of mitochondrial membrane potential

Mitochondrial membrane potential is the transmembrane potential difference resulting from ion concentration differences across biomembrane. As an important indicator of mitochondrial function, MMP can reflect mitochondrial function integrity. The detection of MMP of peaches was carried out according to Baracca et al. (2003). Mitochondria extract (200 μL) as prepared above was added in 3 mL of 10 $mmol\ L^{-1}$ Hepes-HCl buffer (pH 7.4, including 250 $mmol\ L^{-1}$

sucrose, 100 μmol L^{-1} K-EGTA, 2 mmol L^{-1} $MgCl_2$, 4 mmol L^{-1} KH_2PO_4), incubated at 25 °C for 5 min. After adding 0.1 mL of 2 μg mL^{-1} Rh-123, the fluorescence intensity (excitation wavelength 500 nm, emission wavelength 520 nm) was determined after 2 min. One unit of MMP was defined as the ratio of Rh-123 fluorescence quenching (ΔF) to the mitochondrial protein fluorescence intensity (Fi) and the result was expressed as (ΔF/Fi) s^{-1} mg^{-1} protein.

2.2.10. Determination of mitochondrial reactive oxygen species content

The content of mitochondrial reactive oxygen species (ROS) was measured as described as Jing et al. (2016), and expressed as a.u. mg^{-1} protein. The excitation wavelength was 485 nm, and the emission wavelength was 530 nm, respectively.

2.2.11. Effect of H_2O_2 on mitochondrial membranes

The effect of H_2O_2 on mitochondrial membranes in peaches was quantified according to the method of Miyamoto et al. (2008). The control, 5 μmol L^{-1} NO and c-PTIO treatments in the 2nd day were selected for the following experiments. The resuspended mitochondria solution (100 μL) was mixed with 100 μL of H_2O_2 and 100 μL of membrane potential solution to bring the H_2O_2 to a final concentration of 100 μmol L^{-1}. Effect of H_2O_2 on MMP of peaches was measured according to the method of *2.2.10* at 0, 30, 60, and 90 min, respectively.

2.2.12. Determination of mitochondrial membrane permeability

The determination of mitochondrial membrane permeability was done according to the method of Miyamoto et al. (2008). The mitochondrial extract (200 μL) was added to mitochondrial membrane permeability buffer (pH 7.4, including 10.0 mmol L^{-1} Tris-HCl, 125.0 mmol L^{-1} sucrose, 65.0 mmol L^{-1} KCl, 5.0 mmol L^{-1} sodium succinate, 5.0 μmol L^{-1} rotenone) to bring the protein concentration of the mitochondria solution to 500.0 mg L^{-1} in the mixture. After being inverted and mixed well, the solution was heated in a water bath at 37 °C for 120 s and 1.8 mmol L^{-1} $CaCl_2$ solutions were added into the mixture to a final concentration of 50.0 μmol L^{-1} to induce mitochondrial membrane permeability. The mitochondrial suspension had a maximum absorption peak at 540 nm, and the mitochondrial membrane swelling was recorded with the change in absorbance before and after the addition of Ca^{2+} by UV spectrophotometer (UV-2450, Shimadzu, Japan).

2.2.13. Detection of mitochondrial hexokinase activity

The activity of mitochondrial hexokinase was detected according to the method of Majewski et al. (2004). The purified mitochondria (100 μL) was added into 1.5 mL of 41.7 mmol L^{-1} Tris-HCl buffer (pH 8.5, including 7.7 mmol L^{-1} $MgCl_2$, 4.2 mmol L^{-1} glucose, 45 mmol L^{-1} KCl, 0.5 mmol L^{-1} K-EGTA, 6.7 mmol L^{-1} ATP, 0.5 g L^{-1} NADP, 1 U mL^{-1} glucose-6-phosphate dehydrogenase), and the mixture was incubated at 25 °C for 2 min. The activity of hexokinase was determined by monitoring the absorbance at 340 nm (UV-2450, Shimadzu, Japan) for 3 min. One unit of hexokinase activity was defined as the amount of enzyme that produced 1 nmol of hexokinase produced per minute under the assay condition and expressed as U g^{-1} protein.

2.2.14. Fluorescence quenching of NO with PiC and VDAC proteins

The primers of PiC and VDAC (PiC-S 5′-CGCCATATGGCTCTCTCAGAAAAACAC-3′ and PiC-AS 5′-GCGGATCCGTAGAAGGAAGGCGAGTA-3′; VDAC-S 5′-CATATGGTGAAGGGCCCCGGTCTCT-3′ and VDAC-AS 5′-GCGGATCCGTAGAAGGAAGGCGAGTA-3′) with restriction sites of *Nde* I and *Hin*d III, respectively. The genes of PiC and VDAC were initially amplified by PCR from peach mRNA, and the PCR products were cloned into a pMD18-T vector (Takara) according to the manufacturer's instructions. The target genes were verified by sequencing and then ligated into DH5α plasmid by T4 DNA ligase. The recombinant plasmids were transformed into competent *E. coli* Rosetta (DE3) for expression. The recombinant *E. coli* (DE3) strains were inoculated into 25 mL LB medium containing 50 μg mL^{-1} ampicillin and incubated at 37 °C. After the optical density upon reaching OD_{600} = 0.6–0.8, the production proteins were induced by adding isopropyl β-D-1- thiogalactopyranoside (IPTG). The PiC and VDAC were purified as described as Zhao et al. (2018). The HisTrap FF Ni-nitriloacetic acid affinity column was used for purifying PiC and VDAC. PiC and VDAC solution were dissolved in buffer A (pH 7.9, including 1 mol L^{-1} Tris-HCl, 5 mol L^{-1} NaCl, 1 mol L^{-1} imidazole) and injected into the affinity column equilibrated, and then linearly eluted by buffer B (pH 7.9, including 1 mol L^{-1} Tris-HCl, 5 mol L^{-1} NaCl, 1 mol L^{-1} imidazole and 4.8 g carbamide). The purified proteins were renatured by the method of Verlotta and Trono (2014) and then concentrated using an ultracentrifuge tube.

The purified PiC and VDAC proteins were dissolved in 10 mmol L^{-1} pH 7.8 phosphate buffers and purged with nitrogen for 15 min to strip oxygen, respectively. PiC and VDAC protein solution (50 μmol L^{-1}, 10 mL) were added to 1 mL of 0, 250, 500, 1000, 2000 μmol L^{-1} NO solution, respectively. Fluorescence intensity at 380 nm was detected.

2.2.15. Determination of free calcium in mitochondrial

The content of Ca^{2+} was detected according to the method of Chalmers and McCarron (2008). The crude mitochondria were resuspended by 2 mL Mops B. Resuspended mitochondria (200 μL) was mixed with 10 μL of 200 μmol L^{-1} Ca^{2+} fluorescent probe (fura-2 AM), and incubated at 25 °C for 20 min. Then, 100 μL of 10 mmol L^{-1} Hepes-HCl buffer (pH 7.2, including 250 mmol L^{-1} sucrose, 0.1% BSA) was added into the mixture and blended immediately. The mixture was centrifuged at 12000*g* for 5 min at 4 °C. The sediment was collected and resuspended in 800 μL Hepes-HCl buffer. The content of Ca^{2+} in fruit mitochondria was measured by Fluorescence Analysis Instrument (Cary Eclipse, Varian, America), and the excitation wavelength was at 340 nm and 380 nm, respectively, while the fluorescence intensity was measured at 510 nm.

2.2.16. Determination of Ca^{2+} on mitochondrial membrane

The effect of Ca^{2+} on the mitochondrial membrane of peaches was according to the method of Miyamoto et al. (2008). Ca^{2+} solution (1 mol L^{-1}, 1 μL) was added to 100 μL mitochondrial solution to make a concentration of Ca^{2+} of 10 mmol L^{-1} in mitochondrial solution, and then detected the change of fluorescence intensity of Rh-123 for 200 s. Working concentrations of 50 mmol L^{-1} Ca^{2+} concentration were also detected at 200 s, as described above for detecting the change of fluorescence intensity (Cary Eclipse, Varian, America) of Rh-123 after 200 s.

2.3. Data analysis

All experiments were performed in a completely randomized design with three replicates per sample. The data were represented as the mean ± standard deviation of three replicates by analysis of SPSS. Statistical significance was defined as $p < 0.05$, according to the least significant difference (LSD) test.

3. Results

3.1. Changes in firmness

As shown in Fig. 1A, firmness of peaches decreased gradually during storage. Compared with the control, treatments with NO could delay the decrease in the firmness of peaches and treatment with c-PTIO promoted the softening of peaches during storage. The firmness of peaches treated with 15 μmol L^{-1} NO was significantly higher than that of peaches treated with 5 or 30 μmol L^{-1} NO during the 4th to 8th day. Especially in the 8th day, the firmness of peaches of the control was 89.85% as higher as 15 μmol L^{-1} NO treatment. Conversely, firmness of peaches treated by c-PTIO was 89.9% of that of the control. These

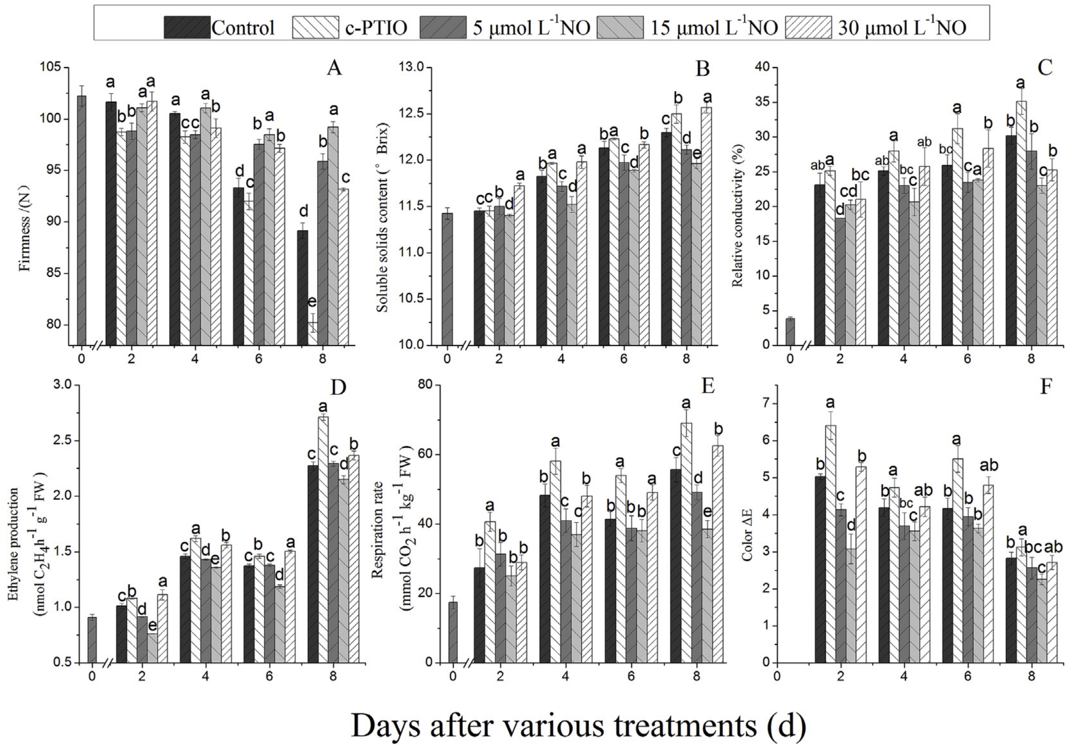

Fig. 1. Effects of different concentrations of NO solutions on firmness (A), soluble solids (B) and relative conductivity (C), ethylene release (D), respiratory rate (E) and color (F) during storage. Each value is presented as mean ± SE (n = 3). Different letters indicate significant differences among different treatments ($P < 0.05$).

results suggested that exogenous NO maintained the firmness of peaches during storage.

3.2. Changes in the contents of soluble solids

Typically, soluble solid content (SSC) in peaches increased during storage as a result of ripening. As shown in Fig. 1B, the treatment with 15 μmol L^{-1} NO significantly delayed the SSC and SSC were lowest in all treatments during the storage. The SSC of peaches treated by 15 μmol L^{-1} NO increased 4.0% over the storage time; however, that of the control and the treatment with c-PTIO increased by 7.6% and 10%, respectively.

3.3. Changes in relative cell membrane conductivity

The relative cell membrane conductivity of peaches treated with 15 μmol L^{-1} NO was the lowest among all treatments during storage (Fig. 1C). The relative cell membrane conductivity of peaches treated with 15 μmol L^{-1} NO was 82.1%, and 76.2% of the control at day 4 and day 8, respectively, whereas treatment with c-PTIO significantly increased conductivity. These results showed that NO protected the cell membrane and delayed the senescence of peaches during storage.

3.4. Changes in ethylene release

The release of ethylene was related to maturity in peaches. As shown in Fig. 1D, treatment with 15 μmol L^{-1} NO significantly delayed the release of ethylene. In the 2nd day, the release of ethylene in peaches treated with 15 μmol L^{-1} NO was 75.2% of the control. On the contrary, c-PTIO treatment increased the release of ethylene. Ethylene production in 15 μmol L^{-1} NO-treated peaches was 2.15 nmol h^{-1} g^{-1} FW and that in c-PTIO-treated peaches was 2.72 nmol h^{-1} g^{-1} FW at day 8, respectively.

3.5. Changes in respiratory rate

The respiration intensity increased as the peaches maturity. As shown in Fig. 1E, the respiration was significantly inhibited by NO. The respiration rate of peaches treated by 15 μmol L^{-1} NO was 9.23% lower than that of the control on day 2. However, the respiration rate of peaches treated with c-PTIO was 14.78% higher than that of the control on the 2nd day. These results showed that treatment with 15 μmol L^{-1} NO significantly delayed the peaches ripening by inhibiting the respiration during storage.

3.6. Changes in color

Treatment with 15 μmol L^{-1} NO affected the total color difference ΔE* of the peaches to a lesser extent than the control and the treatment with c-PTIO. The ΔE* of peaches treated with 15 μmol L^{-1} NO indicated that less browning occurred during storage (Fig. 1F). By contrast, the ΔE* of the control and c-PTIO treatment indicated that more browning occurred during storage. Especially at day 2, the ΔE* of peaches treated by 15 μmol L^{-1} NO was 3.08, while the ΔE* of the control and c-PTIO treated peaches were 5.03 and 6.41, respectively.

3.7. Changes in mitochondrial membrane permeability

During storage, the mitochondrial membrane permeability of peaches increased gradually (Fig. 2A). Mitochondrial membrane resistance was enhanced for 5 μmol L^{-1} and 15 μmol L^{-1} NO treatments compared with the control. Mitochondrial membrane permeability of peaches treated with c-PTIO was 27.01% higher than that of the control at day 6. However, mitochondrial membrane permeability of peaches treated with 15 μmol L^{-1} NO achieved 81.9% of that of the control on day 8. These results suggested that treatment with exogenous NO could significantly alleviate mitochondrial membrane permeability, which might reduce apoptosis.

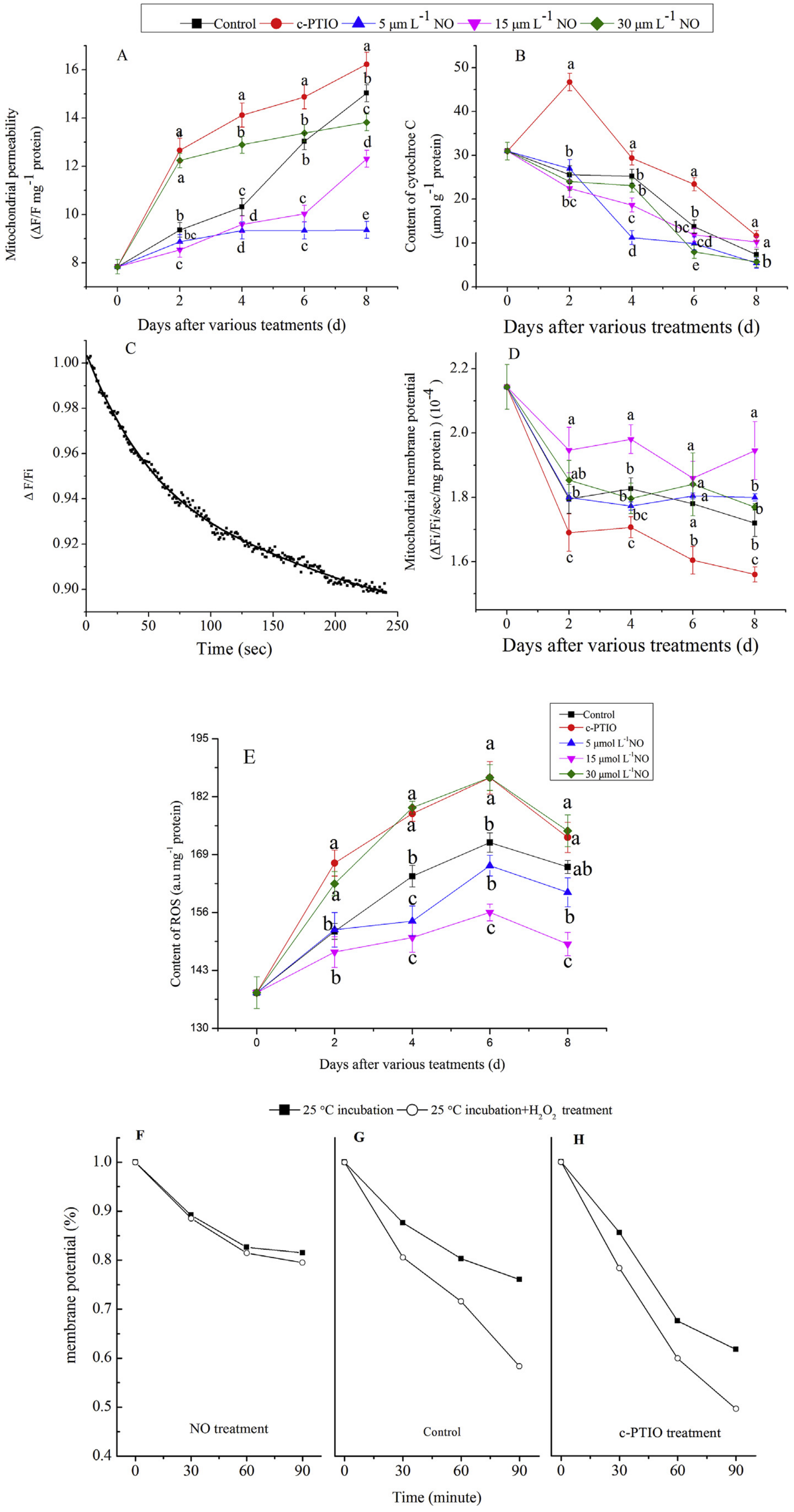

Fig. 2. Effects of different concentrations of NO solutions on mitochondrial permeability (A) and content of cytochrome C (B) during storage. (C) Fluorescence curve of mitochondrial membrane potential monitored by fluorescence quenching of Rhodamine 123. (D) Effects of different concentrations of NO solutions on MMP. (E) Effects of different concentrations of NO solutions on content of ROS. Effects on the ability of permeability transition of mitochondria under oxidative stress of NO treatment (F), control (G) and c-PTIO treatment (H) in peaches storage. Each value is presented as mean ± SE ($n = 3$). Different letters indicate significant differences among different treatments ($P < 0.05$).

3.8. Changes in mitochondrial cytochrome C content

The content of mitochondrial cytochrome C decreased during storage (Fig. 2B). The peaches treated with c-PTIO significantly increased the content of mitochondrial cytochrome C. However, mitochondrial cytochrome C content of peaches treated with 15 μmol L^{-1} NO was about 60.2% and 38.2% of that of the control at day 4 and day 6, respectively. Exogenous NO decreased the release of mitochondrial cytochrome C during storage compared with the control.

3.9. Changes in MMP

Mitochondrial membrane potential (MMP) is the transmembrane potential difference resulting from ion concentration differences across biomembrane. As an important indicator of mitochondrial function, MMP can reflect mitochondrial function integrity. In this study, MMP was characterized by the fluorescence intensity of Rh-123 (Fig. 2C). MMP in peaches generally decreased during storage (Fig. 2D). However, treatment with 15 μmol L^{-1} NO significantly maintained MMP at a high level, while treatment with c-PTIO significantly decreased MMP during storage. MMP of c-PTIO treatment was 9.9% and 9.3% of the control at day 6 and day 8, respectively. However, MMP of peaches treated with 15 μmol L^{-1} NO was 7.41% and 11.51% higher than that of the control at day 4 and day 8, respectively.

3.10. Change in mitochondrial ROS content

The content of ROS in mitochondria of peaches increased during storage (Fig. 2E). The peaches treated by c-PTIO significantly increased the content of ROS. On the 6th day, the content of ROS in peaches treated with 15 μmol L^{-1} NO was 156.03 a.u mg^{-1} protein and that treated with c-PTIO was 186.22 a.u mg^{-1} protein. As shown in Fig. 2E, the content of ROS in peaches treated with 30 μmol L^{-1} NO was significantly higher than that of the control during storage, while that of peaches treated with 15 μmol L^{-1} NO was lower than that of the control.

3.11. Changes in the effect of H_2O_2 on MMP

Mitochondrial calcium overload, oxidative stress, increased phosphate concentrations, and adenylated consumption can induce MPTP opening. Samples not exposed to hydrogen peroxide under a constant temperature of 25 °C were used as a reference. As shown in Fig. 2 F−H, mitochondrial oxidative stress caused by hydrogen peroxide on peaches could induce membrane depolarization, and H_2O_2 could be seen to accelerate the pore opening. As shown in Fig. 2F, the membrane potential of mitochondria decreased after 90-min exposure to 100 mmol L^{-1} H_2O_2. Compared with the control, treatment with NO inhibited the membrane potential depolarization caused by H_2O_2 (Fig. 2G), whereas peaches treated with c-PTIO accelerated the MPTP opening (Fig. 2H). Thus, NO treatment inhibited the decrease of membrane potential induced by oxidative stress. Oxidative stress also changed the voltage dependence of MPTP as well as allowed the pore to open at more negative potentials. The inhibitory effect of NO on oxidative stress-induced MPTP opening might be related to NO depletion of ROS, as NO could act as an antioxidant to protect mitochondrial membranes from oxidative damage.

3.12. Changes in mitochondrial hexokinase activity

The activity of hexokinase in peaches was significantly increased during storage (Fig. 3A). Specifically, hexokinase activities of treatment with 15 μmol L^{-1} NO were 57.26% higher than that of the control at day 2. However, the activity of hexokinase for the c-PTIO treatment was 16.1% lower than that of the control and 56.7% lower than that of treatment with NO on day 8.

3.13. Fluorescence quenching effect of NO with PiC and VDAC proteins

The quenching reaction involves physical contact between the quencher and a protein and can be kinetically described in terms of a collisional and a static component. Static quenching is readily detected in proteins that are denatured or contain only a single fluorophor. This probe technique is used for monitoring protein conformational changes (Eftink and Ghiron, 1976). The interaction of PiC with NO produced a non-fluorescent complex with a specific structure that resulted in fluorescence quenching. Fluorescence quenching took place after the addition of NO solution into PiC solution. The fluorescence intensity of the solution was only 27.1% of the pure protein solution when the concentration of NO solution was 2 mmol L^{-1}. This was consistent with the decreased fluorescent intensity observed after the molecules of PiC and NO were combined which was described by Lineweaver-Burk (Mao et al., 2002):

$$(F_0-F)^{-1} = (F_0)^{-1} + (KF_0C_q)^{-1} \tag{1}$$

Where F_0 is the fluorescence intensity of PiC protein without the addition of NO, F is the fluorescence intensity, and C_q is the concentration of NO. The corresponding double reciprocal map was shown in Fig. 3B. These results confirmed a regulation about static quenching, which indicated that the combination of NO and PiC results in decreasing protein fluorescence intensity. It suggested that NO and PiC formed a complex through the hydrogen bonds.

The Scatchard model was used to analyze the binding molar ratio and apparent binding constant of the reaction of PiC protein with NO (Naik et al., 1975). Assuming that a PiC protein molecule had n binding sites of NO, the following reactions occurred:

$$\mathrm{PiC} + n\mathrm{NO} = \mathrm{PiC} - \mathrm{NOn} \tag{2}$$

The chemical equilibrium constant of this reaction formula could be expressed as:

$$K = [\mathrm{PiC}-\mathrm{NO}_n]/[\mathrm{PiC}][\mathrm{NO}]^n \tag{3}$$

K is an apparent binding constant, [PiC] and [NO] are the free concentrations of PiC and NO respectively, and [PiC-NO] is the amount of fluorescence in the complexed form, assuming that the bound complexes NO-PiC complexes do not fluoresce, as expressed by (3),

$$\Delta F/F = [\mathrm{PiC}-\mathrm{NO}_n]/[\mathrm{PiC}] = K[\mathrm{NO}]^n \tag{4}$$

Where ΔF is a difference of fluorescence intensity between initial fluorescence intensity and when NO was added, the expression could be rewritten as:

$$\log[\Delta F/F] = \log K + n\log[\mathrm{NO}] \tag{5}$$

Changing the concentration of NO and fixing the concentration of PiC protein to detect the changes in fluorescence at 380 nm (Fig. 3C). PiC and NO could mainly form 1:1 complex in the changes of NO concentration condition by calculating the slope and intercept ($n = 1$).

The method in detecting fluorescence quenching effect of NO and VDAC protein was the same as PiC. The fluorescence intensity of the solution was only 68.36% of the pure protein solution when the concentration of NO solution was 1.2 mmol L^{-1}. Changing the concentration of NO and fixing the concentration of VDAC protein to detect the changes in fluorescence at 380 nm (Fig. 3E). VDAC and NO could mainly form 1:1 complex in the changes of NO concentration condition by calculating the slope and intercept ($n = 1$).

3.14. Changes in free Ca^{2+} in mitochondrial matrix

Peaches treated with 15 μmol L^{-1} NO had higher Ca^{2+} content compared with the control during storage. (Fig. 4A). Free Ca^{2+} levels in the mitochondrial matrix of peaches treated with c-PTIO were 11.1% and 22.6% lower than that of the control on day 6 and day 8, respectively. The free Ca^{2+} content in the mitochondrial matrix of peaches

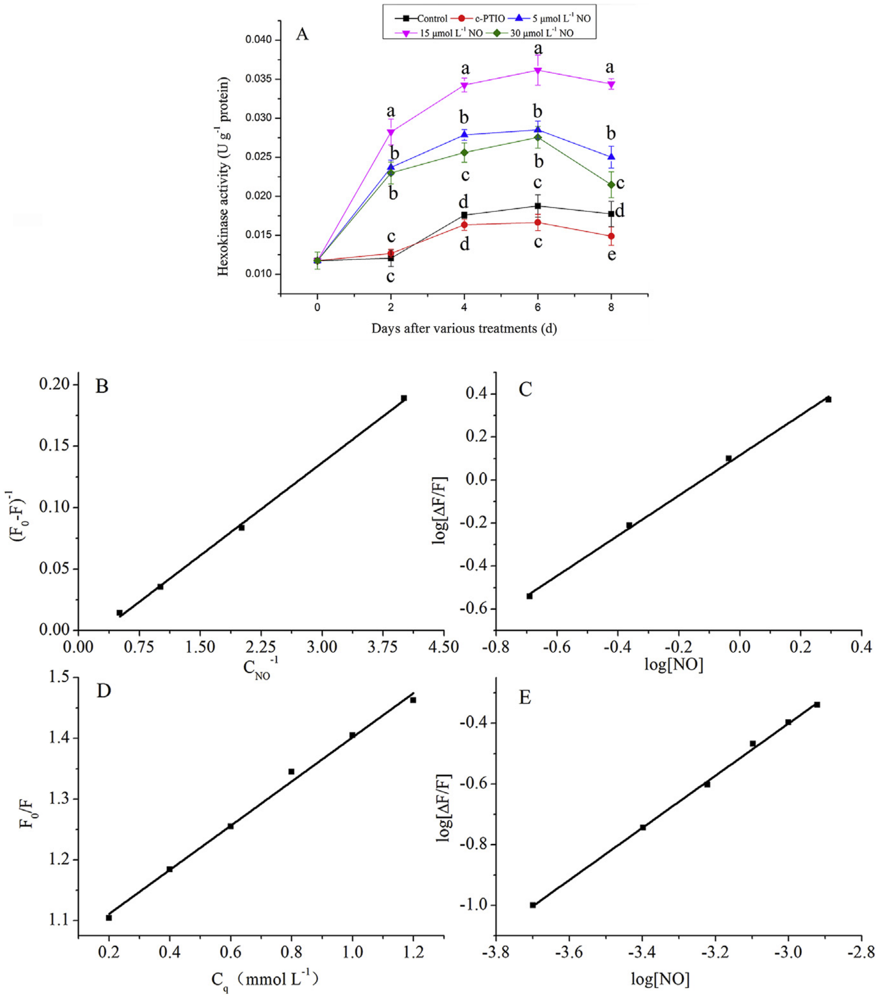

Fig. 3. (A) Effects on hexokinase activities in peaches treated with different concentrations of NO solutions during storage. Lineweaver-Burk double-reciprocal curves of NO vs. PiC (B), VDAC (D) protein and Plot of log [ΔF/F] vs. PiC (C), VDAC (E) log [NO], Each value is presented as mean ± SE (n = 3). Different letters indicate significant differences among different treatments ($P < 0.05$).

treated with 15 μmol L^{-1} NO significantly was higher than that of the control at day 2. Removal of endogenous NO significantly accelerated the outflow of Ca^{2+} from the mitochondrial matrix, indicating MPTP could restrict the passage of small molecules and regulate mitochondrial Ca^{2+} homeostasis.

3.15. Changes in the effect of Ca^{2+} on MMP

The changes in fluorescence intensity via induced depolarization of the membrane with exogenous Ca^{2+} were used for real-time monitoring with mitochondrial Rh-123-loaded fluorescence spectrophotometry (Fig. 4B, C, and D). Exogenous Ca^{2+} at 10 mmol L^{-1}did not cause substantial changes in mitochondrial membrane potential in both the control and NO treatment (Fig. 4C), whereas 10 mmol L^{-1} Ca^{2+} was found to increase the fluorescence intensity in the c-PTIO treatment (Fig. 4D). The fluorescence intensity was increased in all treatments when 50 mmol L^{-1} exogenous Ca^{2+} was inducted. The increase in the fluorescence intensity of the treatment with c-PTIO was significant; however, that of treatment with NO was not great. These indicated that the opening of MPTP was influenced to different degrees depending on NO in the presence of 50 mmol L^{-1} Ca^{2+}, suggesting that NO could inhibit the induction of mitochondrial depolarization by Ca^{2+}. The capacity of mitochondria Ca^{2+} decreased after clearance the endogenous NO, and it was difficult to maintain MMP after adding the high concentration of exogenous Ca^{2+}.

4. Discussion

Firmness and soluble solids contents are major physiological and biochemical parameters of peaches during storage, which are influenced by maturation. Compared with other treatments, the decrease in the firmness and the increase in soluble solids contents were delayed in peaches treated with 15 μm L^{-1} NO (Fig. 1A and B). Conductivity can be used to measure cell membrane permeability, and treatment with 15 μmol L^{-1} NO decreased the relative conductivity of peaches during storage. However, peaches treated by c-PTIO increased the relative conductivity (Fig. 1C). Both NO and ethylene are specific signal molecules in fruit ripening. Ethylene is a key molecule to quality preservation during fruit ripening, and NO is a signal molecule regulating fruit ripening (Corpas and Palma, 2018; Yang et al., 2016). The ethylene biosynthesis can be regulated by NO during fruit ripening (Mukherjee, 2019). In this experiment, the release of ethylene and the rate of respiration of peaches were delayed by treatment with 15 μmol L^{-1} NO during storage (Fig. 1 DE), indicating that NO could slow down the senescence of peaches by inhibiting endogenous ethylene and the rate of respiration, thereby to prolong the storage time of peaches at room temperature. This paper indicated that high concentration of NO (30 μmol L^{-1} NO) had high and toxic to peaches, low concentration of NO (5 μmol L^{-1} NO) might be too low to trigger the changes of peaches. Treatments with 15 μmol L^{-1} NO showed effective preservation for peaches.

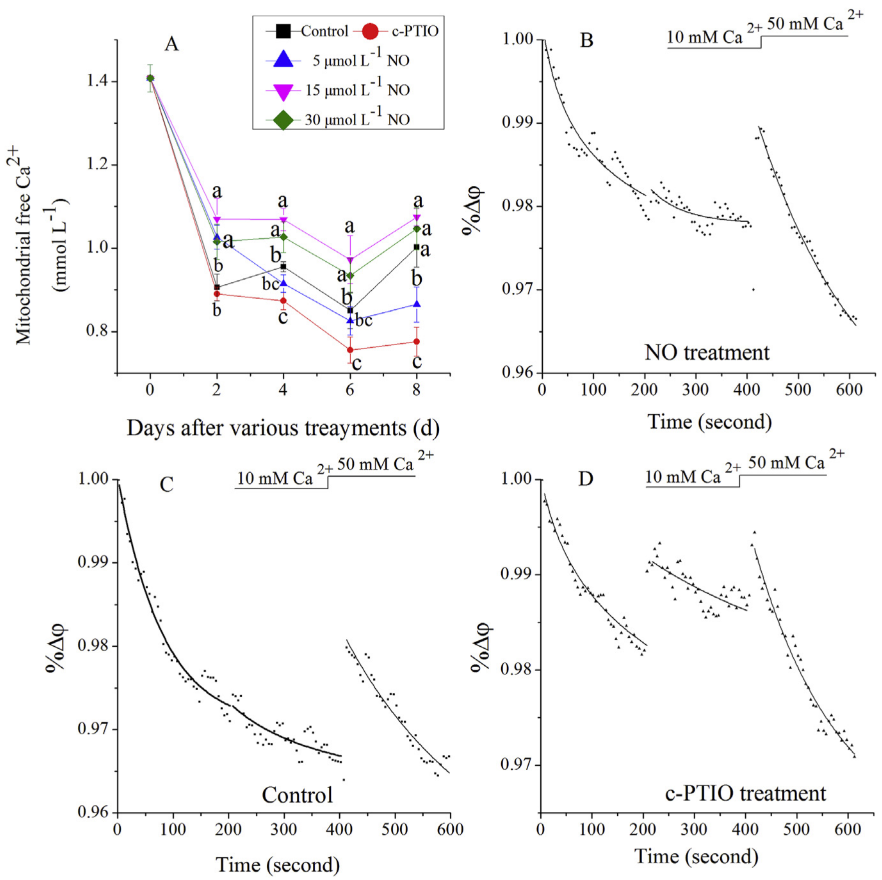

Fig. 4. (A) Effects on the free Ca^{2+} in mitochondrial matrix treated with different concentrations of NO solutions in peaches during storage. Effects on the Ca^{2+}-induced mitochondrial membrane depolarization of NO treatment (B), control (C) and c-PTIO treatment (D) in peaches storage. Each value is presented as mean ± SE (n = 3). Different letters indicate significant differences among different treatments ($P < 0.05$).

The mitochondrial membrane permeability transition of peaches during cold storage could be delayed by exogenous 15 μmol L^{-1} NO and promoted by c-PTIO (Jing et al., 2016). Membrane permeability of mitochondria with NO treatment remained at a relatively low level during storage (Fig. 2A). As shown in Fig. 2D, MMP decreased gradually, indicating that the exogenous NO can prolong the storage by upregulating mitochondrial membrane permeability. Cytochrome C is a protein located on the mitochondrial membrane which terminates functionally upon binding with acidic phospholipids in the MIM as a catalyst for apoptosis (Thong and Tsoukanova, 2018). Cytochrome C can be released from mitochondria into the cytoplasm through MPTP (Wang et al., 2017). As shown in Fig. 2B, mitochondrial cytochrome C content decreased during storage. With the extension of storage, the permeability of the mitochondrial membrane increased. Swelling and junction cleavage lead to disruption of mitochondrial membrane structure, releasing more cytochrome C, and then increased ROS in intracellular. Thus, the low content of cytochrome C meant the low release of cytochrome *c*, which could maintain cell survival and reduce the generation of ROS, thereby prolonging peach preservation.

The activity of hexokinase was highest in peaches treated with 15 μmol L^{-1} NO during storage (Fig. 3A). The fluorescence analysis showed that the fluorescence intensity of the VDAC protein solution could be decreased and even quenched by NO. Scatchard model analysis indicated that the protein VDAC could form a 1:1 complex with NO. The result of quenching fluorescence indicated that NO could enter the hydrophobic pores of the VDAC protein and bind to the VDAC protein, due to the strong permeability and lipid solubility of NO (Wink and Mitchell, 1998). MMP could be affected by NO, as fluorescence spectroscopy indicated that NO and VDAC proteins form complexes, and the permeability of MOM was changed by affecting VDAC protein. NO can regulate the redox signal by nitrosylation with the thiol group of the protein, affecting the activity of the protein in the cell (Benhar et al., 2009). The fluorescence analysis showed that NO could quench the intensity of the PiC protein solution. The result from Scatchard model analysis showed the protein of PiC could form a 1:1 complex with NO. PiC could be *S*-nitrosylated by NO. *S*-nitrosylation is an important cellular regulatory mechanism, which is a reversible post-translational protein modification, compared to phosphorylation, acylation, and nitration. The contents of Ca^{2+} were decreased rapidly at the early stage of storage and then stabilized (Fig. 4A). Mitochondria treated with 15 μmol L^{-1} NO had high tolerances of Ca^{2+} and H_2O_2; however, mitochondria treated with c-PTIO conferred minimal resistance. MMP was hardly affected in the peaches treated with a low concentration of Ca^{2+} and 15 μmol L^{-1} NO. (Fig. 4B, C, D). The mitochondria of peaches treated by NO were reduced after adding a high concentration of Ca^{2+}. The opening of the CypD-dependent MPTP can be induced by oxidative effects of H_2O_2, and NO can induce CypD protein *S*-nitrosylation, thereby reducing CypD activation and inhibiting MPTP opening (Nguyen et al., 2011). These indicated that treatment with NO could maintain the MMP, prevent the dissipation of MMP and inhibit the outflow of Ca^{2+} in mitochondria, thus prolonging the storage of peaches.

Exogenous NO could effectively protect the harvested peach fruit and prolong its shelf life. The mitochondrial antioxidant system played important roles in maintaining the normal physiological activities of cells. NO at 15 μmol L^{-1} could maintain the stability of the mitochondrial membrane structure and regulate the normal physiological process of the MPTP.

5. Conclusion

Exogenous NO maintained a high level of MMP and mitochondrial membrane permeability, a high tolerance of Ca^{2+} and H_2O_2, and increased hexokinase activity and decreased the content of cytochrome C during storage. However, treatment with c-PTIO unbalanced the potential of the mitochondrial membrane. It indicated that treatment with NO could maintain the MMP, prevent the dissipation of MMP during storage, and inhibit the outflow of Ca^{2+} in mitochondria, thereby prolonging the storage of peaches.

Conflicts of interest

The authors confirm that this article content has no conflict of interest.

Author contributions

Shuhua Zhu and Jianrong Feng designed the research. Dandan Huang and Shan Hu performed the research. Shan Hu and Dandan Huang made equal contributions to this work. All authors read and approved the final version of the paper.

Acknowledgements

This work was supported by the National Natural Science Foundation of China (31270723, 31770724).

References

Baracca, A., Sgarbi, G., Solaini, G., Lenaz, G., 2003. Rhodamine 123 as a probe of mitochondrial membrane potential: evaluation of proton flux through F_0 during ATP synthesis. Biochim. Biophys. Acta Bioenerg. 1606, 137–146. https://doi.org/10.1016/S0005-2728(03)00110-5.

Benhar, M., Forrester, M.T., Stamler, J.S., 2009. Protein denitrosylation: enzymatic mechanisms and cellular functions. Nat. Rev. Mol. Cell Biol. 10, 721–732. https://doi.org/10.1038/nrm2764.

Bhattacharya, A., Biswas, P., Kar, P., Roychoudhury, P., Basu, S., Ganguly, S., Ghosh, S., Panda, K., Pal, R., Dasgupta, A.K., 2017. Nitric oxide sensing by chlorophyll a. Anal. Chim. Acta 985, 101–113. https://doi.org/10.1016/j.aca.2017.07.026.

Chalmers, S., McCarron, J.G., 2008. The mitochondrial membrane potential and Ca^{2+} oscillations in smooth muscle. J. Cell Sci. 121, 75–85. https://doi.org/10.1242/jcs.014522.

Corpas, F.J., Palma, J.M., 2018. Nitric oxide on/off in fruit ripening. Plant Biol. 20, 805–807. https://doi.org/10.1111/plb.12852.

Correa-Aragunde, N., Foresi, N., Lamattina, L., 2015. Nitric oxide is a ubiquitous signal for maintaining redox balance in plant cells: regulation of ascorbate peroxidase as a case study. J. Exp. Bot. 66, 2913–2921. https://doi.org/10.1093/jxb/erv073.

Domingos, P., Prado, A.M., Wong, A., Gehring, C., Feijo, J.A., 2015. Nitric oxide: a multitasked signaling gas in plants. Mol. Plant 8, 506–520. https://doi.org/10.1016/j.molp.2014.12.010.

Eftink, M.R., Ghiron, C.A., 1976. Exposure of tryptophanyl residues in proteins. Quantitative determination by fluorescence quenching studies. Biochemistry 15, 672–680. https://doi.org/10.1021/bi00648a035.

Ellenrieder, L., Rampelt, H., Becker, T., 2017. Connection of protein transport and organelle contact sites in mitochondria. J. Mol. Biol. 429, 2148–2160. https://doi.org/10.1016/j.jmb.2017.05.023.

Gupta, A.K., Kumari, A., Mishra, S., Wany, A., Gupta, K.J., 2016. The functional role of nitric oxide in plant mitochondrial metabolism. Adv. Bot. Res. 77, 145–163. https://doi.org/10.1016/bs.abr.2015.10.007.

Haferkamp, I., Schmitz-Esser, S., 2012. The plant mitochondrial carrier family: functional and evolutionary aspects. Front. Plant Sci. 3, 2. https://doi.org/10.3389/fpls.2012.00002.

Igamberdiev, A.U., Ratcliffe, R.G., Gupta, K.J., 2014. Plant mitochondria: source and target for nitric oxide. Mitochondrion 19, 329–333. https://doi.org/10.1016/j.mito.2014.02.003.

Jing, G., Zhou, J., Zhu, S., 2016. Effects of nitric oxide on mitochondrial oxidative defence in postharvest peach fruits. J. Sci. Food Agric. 96, 1997–2003. https://doi.org/10.1002/jsfa.7310.

Kühlbrandt, W., 2015. Structure and function of mitochondrial membrane protein complexes. BMC Biol. 13, 89. https://doi.org/10.1186/s12915-015-0201-x.

Majewski, N., Nogueira, V., Bhaskar, P., Coy, P.E., Skeen, J.E., Gottlob, K., Chandel, N.S., Thompson, C.B., Robey, R.B., Hay, N., 2004. Hexokinase-mitochondria interaction mediated by Akt is required to inhibit apoptosis in the presence or absence of Bax and Bak. Mol. Cell 16, 819–830. https://doi.org/10.1016/j.molcel.2004.11.014.

Mao, H., Yang, T., Cremer, P.S., 2002. Design and characterization of immobilized enzymes in microfluidic systems. Anal. Chem. 74, 379–385. https://doi.org/10.1021/ac010822u.

Margoliash, E., Frohwirt, N., 1959. Spectrum of horse-heart cytochrome c. Biochem. J. 71, 570–572. https://doi.org/10.1042/bj0710570.

Millar, A.H., Liddell, A., Leaver, C.J., 2001. Isolation and subfractionation of mitochondria from plants. Methods Cell Biol. 65, 65–90. https://doi.org/10.1016/S0091-679X(01)65004-0.

Miyamoto, S., Murphy, A.N., Brown, J.H., 2008. Akt mediates mitochondrial protection in cardiomyocytes through phosphorylation of mitochondrial hexokinase-II. Cell Death Differ. 15, 521–529. https://doi.org/10.1038/sj.cdd.4402285.

Mukherjee, S., 2019. Recent advancements in the mechanism of nitric oxide signaling associated with hydrogen sulfide and melatonin crosstalk during ethylene-induced fruit ripening in plants. Nitric Oxide 82, 25–34. https://doi.org/10.1016/j.niox.2018.11.003.

Naik, D.V., Paul, W.L., Schulman, S.G., 1975. Fluorometric determination of drug-protein association constants: binding of pamaquine by bovine serum albumin. J. Pharmaceut. Sci. 64, 1677–1680. https://doi.org/10.1002/jps.2600641020.

Nguyen, T.T., Stevens, M.V., Kohr, M., Steenbergen, C., Sack, M.N., Murphy, E., 2011. Cysteine 203 of cyclophilin D is critical for cyclophilin D activation of the mitochondrial permeability transition pore. J. Biol. Chem. 286, 40184–40192. https://doi.org/10.1074/jbc.M111.243469.

Perez, M.J., Quintanilla, R.A., 2017. Development or disease: duality of the mitochondrial permeability transition pore. Dev. Biol. 426, 1–7. https://doi.org/10.1016/j.ydbio.2017.04.018.

Scheler, C., Durner, J., Astier, J., 2013. Nitric oxide and reactive oxygen species in plant biotic interactions. Curr. Opin. Plant Biol. 16, 534–539. https://doi.org/10.1016/j.pbi.2013.06.020.

Sehrawat, A., Gupta, R., Deswal, R., 2013. Nitric oxide-cold stress signalling cross-talk, evolution of a novel regulatory mechanism. Proteomics 13, 1816–1835. https://doi.org/10.1002/pmic.201200445.

Singh, S.P., Singh, Z., Swinny, E.E., 2009. Postharvest nitric oxide fumigation delays fruit ripening and alleviates chilling injury during cold storage of Japanese plums (*Prunus salicina* Lindell). Postharvest Biol. Technol. 53, 101–108. https://doi.org/10.1016/j.postharvbio.2009.04.007.

Song, J., Li, Y., Song, J., Hou, F., Liu, B., Li, A., 2017. Mangiferin protects mitochondrial function by preserving mitochondrial hexokinase-II in vessel endothelial cells. Biochim. Biophys. Acta (BBA) - Mol. Basis Dis. 1863, 1829–1839. https://doi.org/10.1016/j.bbadis.2017.05.001.

Tewari, D., Ahmed, T., Chirasani, V.R., Singh, P.K., Maji, S.K., Senapati, S., Bera, A.K., 2015. Modulation of the mitochondrial voltage dependent anion channel (VDAC) by curcumin. Biochim. Biophys. Acta Biomembr. 1848, 151–158. https://doi.org/10.1016/j.bbamem.2014.10.014.

Thong, A., Tsoukanova, V., 2018. Cytochrome-c-assisted escape of cardiolipin from a model mitochondrial membrane. Biochim. Biophys. Acta Biomembr. 1860, 475–480. https://doi.org/10.1016/j.bbamem.2017.10.032.

Verlotta, A., Trono, D., 2014. Expression, purification and refolding of active durum wheat (*Triticum durum* Desf.) secretory phospholipase A2 from inclusion bodies of *Escherichia coli*. Protein Expr. Purif. 101, 28–36. https://doi.org/10.1016/j.pep.2014.05.009.

Wang, L.L., Han, L., Ma, X.L., Yu, Q.L., Zhao, S.N., 2017. Effect of mitochondrial apoptotic activation through the mitochondrial membrane permeability transition pore on yak meat tenderness during postmortem aging. Food Chem. 234, 323–331. https://doi.org/10.1016/j.foodchem.2017.04.185.

Wink, D.A., Mitchell, J.B., 1998. Chemical biology of nitric oxide: insights into regulatory, cytotoxic, and cytoprotective mechanisms of nitric oxide. Free Radic. Biol. Med. 25, 434–456. https://doi.org/10.1016/S0891-5849(98)00092-6.

Wu, H.Y., Huang, C.H., Lin, Y.H., Wang, C.C., Jan, T.R., 2018. Cannabidiol induced apoptosis in human monocytes through mitochondrial permeability transition pore-mediated ROS production. Free Radic. Biol. Med. 124, 311–318. https://doi.org/10.1016/j.freeradbiomed.2018.06.023.

Yang, Y., Zheng, Y., Liu, C., Chen, L., Ma, J., Sheng, J., Shen, L., 2016. Inhibition of nitric oxide synthesis delayed mature-green tomato fruits ripening induced by inhibition of ethylene. Sci. Hortic. 211, 95–101. https://doi.org/10.1016/j.scienta.2016.07.026.

Yarlagadda, K., Hassani, J., Foote, I.P., Markowitz, J., 2017. The role of nitric oxide in melanoma. Biochim. Biophys. Acta Rev. Canc. 1868, 500–509. https://doi.org/10.1016/j.bbcan.2017.09.005.

Yu, M., Lamattina, L., Spoel, S.H., Loake, G.J., 2014. Nitric oxide function in plant biology: a redox cue in deconvolution. New Phytol. 202, 1142–1156. https://doi.org/10.1111/nph.12739.

Zhao, W., Liu, L., Du, G., Liu, S., 2018. A multifunctional tag with the ability to benefit the expression, purification, thermostability and activity of recombinant proteins. J. Biotechnol. 283, 1–10. https://doi.org/10.1016/j.jbiotec.2018.07.005.

Zhu, S., Liu, M., Zhou, J., 2006. Inhibition by nitric oxide of ethylene biosynthesis and lipoxygenase activity in peach fruit during storage. Postharvest Biol. Technol. 42, 41–48. https://doi.org/10.1016/j.postharvbio.2006.05.004.